UNIVERSITY OF SÃO PAULO
SÃO CARLOS SCHOOL OF ENGINEERING

Gabriel José Negrelli Gomes

Development of Software for Wind Power System Model Identification

São Carlos

2019

Gabriel José Negrelli Gomes

Development of Software for Wind Power System Model Identification

Dissertation submitted to the São Carlos School of Engineering of the University of São Paulo in partial fulfillment of the requirements for the degree of Master of Science in Electrical Engineering.

Area: Electrical Power Systems

Supervisor: Prof. Dr. Elmer Pablo Tito Cari

São Carlos

2019

ABSTRACT

GOMES, G. J. N. **Model for theses and dissertations in LaTeX using the USPSC class to the EESC**. 2019. 34p. Dissertation (Masters) - São Carlos School of Engineering, University of São Paulo, São Carlos, 2019.

This project proposes the development of a software for non-linear system's model identification, focusing on wind power plants. The chosen model for wind power plants is well-known in the literature and is capable of representing the most common wind turbine type during both steady-state and transients. The method applied to identify the model is composed of two optimization algorithms. At the begining of the process, an heuristic approach based on Mean-Variance Mapping Optimization is used in order to reduce the parameter's search region around a possible solution. Afterward, a non-linear algorithm based on Trajectory Sensitivity is used to fine-tune the parameters. The method validation will be made using data from simulated systems. Also, a guided user interface will be developed for this application, aiding new users. All coding for this project will be made in Python.

Keywords: Model identification. Wind power plants. MVMO. Trajectory sensitivity. Python.

RESUMO

GOMES, G. J. N. **Development of Software for Wind Power System Model Identification**. 2019. 34p. Dissertation (Masters) - São Carlos School of Engineering, University of São Paulo, São Carlos, 2019.

O presente trabalho propõe o desenvovlimento de um *software* voltado para a identificação de modelos de sistemas não-lineares, com enfoque em plantas eólicas. O modelo escolhido para plantas eólicas é bem consolidado na literatura, sendo capaz de representar o comportamento de geradores mais utilizados nas instalações deste tipo tanto durante o regime permanente quanto em transitórios. O método utilizado para a identificação do modelo é constituído por dois algoritmos de otimização. Primeiramente, é empregada uma abordagem heurística, baseada em Otimização por Mapeamento de Média-Variância, a fim de reduzir a região de busca dos parâmetros em torno de uma possível solução. Em seguida, lança-se mão de um algoritmo não-linear, baseado no Método de Sensibilidade de Trajetória, para realizar os ajustes finais nos valores dos parâmetros. A validação do método será feita utilizando medidas de sistemas simulados. Com o intuito de facilitar a experiência do usuário com o programa, será desenvolvida uma interface gráfica para o *software*. Tanto as rotinas para identificação de modelos quanto a interface gráfica serão desenvolvidas em Python.

Palavras-chave: Identificação de modelos. Plantas eólicas. MVMO. Sensibilidade de trajetória. Python.

LIST OF FIGURES

LIST OF ABBREVIATIONS AND ACRONYMS

ABEEólica	Associação Brasileira de Energia Eólica
ANEEL	Agência Nacional de Energia Elétrica
DFIG	Doubly Fed Induction Generator
EESG	Electrical Excited Synchronous Generator
EU	European Union
IEEE	Institute of Electrical and Electronics Engineers
MVMO	Mean-Variance Mapping Optimization
PMSG	Permanent Magnet Synchronous Generator
PROINFA	Program of Incentive to Alternative Electric Energy Sources
SCIG	Squirrel Cage Induction Generator
TS	Trajectory Sensitivity Method
US	United States of America
UK	United Kingdom
WECC	Western Electricity Coordinating Council
WRIG	Wound Rotor Induction Generator
WTG	Wind Turbine Generator

CONTENTS

1 INTRODUCTION

During the last decade, the world has seen an increase in participation of renewable sources in power generation, leaded mainly by wind and solar energy. These green technologies provide an alternative to sources based on fossil fuel, lowering pollution levels and reducing greenhouse gas emissions. On the other hand, the power output from these sources rely on weather conditions and can't be fully controlled.

This increase is seen worldwide, as part of policies to reduce the human impact on climate and the environment. This 'renewable wave' is leaded mainly by European countries, specially in the European Union (EU), United States (US) and China. In particular, EU has set in 2010 a strategy plan to reduce its greenhouse emissions by at least 20% compared to 1990 levels and increase the share of renewable sources to at least 20% by 2020 (Commission European, 2010).

Brazil does not lag far behind EU regarding renewable sources policies. In 2002, the country passed a bill that, among other actions, creates the Program of Incentive to Alternative Electric Energy Sources (PROINFA). This program aims to increase the share of wind, solar, small hydro and biomass energy production. The final goal is to have these resources corresponding to 10% of Brazil's annual energy consumption (Federative Republic of Brazil, 2002).

1.1 Wind Energy

Those policies stimulated the increase of wind energy participation, reaching a scenario where it is the main energy source of some countries. In the EU, wind energy alone generated 362 TWh in 2018, covering 14% of the electricity demand, a share 2% higher than 2017. Breaking down to countries, Denmark leads in this sector, with 41% of its demand supplied by wind power plants, followed by Ireland (28%), Portugal (24%) and Germany (21%). The total installed capacity across the 28 EU countries is 178.8 GW, with Germany in first position, with a total installed capacity of 59.3 GW, followed by Spain and the United Kingdom (UK), with 23.5 and 21.0 GW installed, respectively (Wind Europe, 2019). Figure 1 displays the detailed percentage of electricity demand covered by wind in the EU.

In Brazil, wind energy contributed with 42.4 TWh during 2017, resulting in a participation share of 7.2%. But, while other sources, such as hydro and coal, had its share lowered, wind energy had the highest variation among sources comparing to 2016, increasing its contribution by 26.5% (EPE, 2018). In therms of installed capacity, wind power plants appear in 2nd place, with 14.7 GW installed, only behind hydro power plants

Figure 1: Share of electricity demand in the EU covered by wind energy

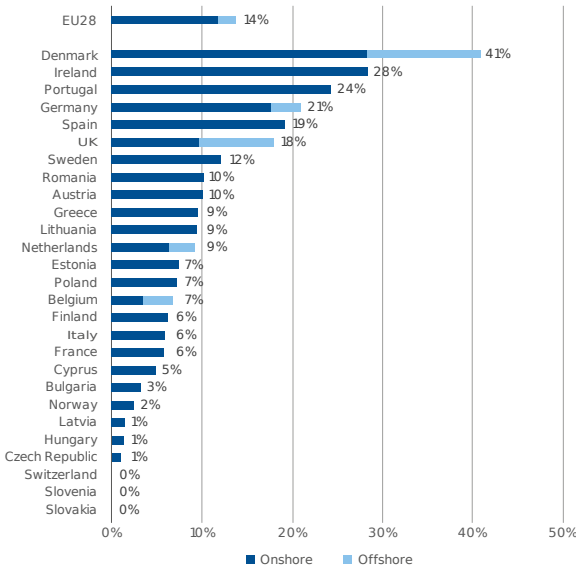

Source: Wind Europe

(ABEEOLICA, 2018), as shown in Figure 2.

However, there is plenty of energy yield for this source to be explored. Studies show that Brazil has potential to generate 272.2 TWh per year, with an installed capacity of 143.5 GW. The Northeast Region has the higher potential, with an annual energy yield of 144.3 TWh and potential to host up to 75.0 GW (AMARANTE et al., 2001). Also, the wind regime in the Northeast Region is complimentary to the water regime of the main river responsible to power generation in the region, as presented by Figure 3. This

Figure 2: Electricity generation in Brazil by source

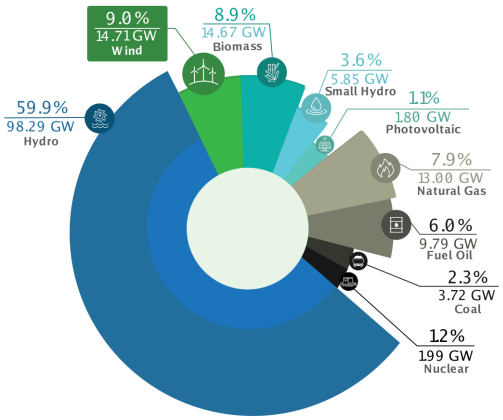

Source: ABEEólica

Figure 3: Wind and water regime in the Northeast Region

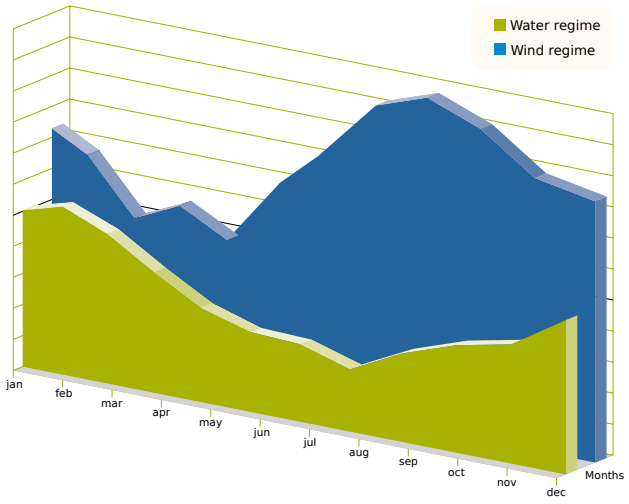

Source: ANEEL

characteristic would help controlling reservoir water level during dry season, an important resource not only for power generation, but also irrigation of crops and water supply (ANEEL, 2005).

With all this information in hand, it is only reasonable to assume that wind energy will increase its participation in electricity generation. But, in order to allow this growth, studies about how wind generators and power plants behave during faults in the grid are needed.

1.2 Wind Turbine Model

With a growing share of energy covered by wind, system operators must consider how wind turbines affect the system stability during faults and maneuvers. To do so, mathematical models capable of describing these machines' behaviour are crucial. Obtaining these models, on the other hand, is not an easy task, due to considerable amount of wind turbines in large power plants, with different manufacturers, technologies, sizes, distances from point of connection and wind conditions. Thus, a model that describes well a particular turbine in a power plant, won't necessarily work for its neighboring generators. Also, due to industrial secrecy, manufacturers provide little or no information about how their turbines behave. Furthermore, having one model for every wind turbine within a power plant would result in a mathematical problem with high complexity and computational cost (ERLICH et al., 2012).

To address this problem, studies such as (MULJADI; ELLIS, 2008), (ELLIS et al., 2011), (COUNCIL, 2008) and (ASMINE et al., 2011), motivated specially by the Institute of Electrical and Electronics Engineers (IEEE) and the Western Electricity Coordinating

Council (WECC), developed generic models able to predict the behaviour of entire wind power plants. Such models reduced the problem complexity, since they were composed of a single equivalent generator. A two-machine model is needed only in rare cases, such as when the wind power plant is composed of two or more types of wind turbines (ELLIS et al., 2011).

These studies have also shown that commercial wind turbine generators (WTG) could be sorted into four basic types, according to its technology (ELLIS et al., 2011). These types are described in the following subsections.

1.2.1 Type-1 Wind Turbine Generator

The first type of wind turbine generator is composed of a Squirrel Cage Induction Generator (SCIG) connected to a wind turbine through a controlled gearbox, as displayed in Figure 4. Due to its torque-speed characteristics, generators of this type operate at constant rotor speed, requiring robust controllers on gearbox and blade. Besides, as usual to any induction generator, the SCIG absorbs reactive power during operation. Thus, capacitors are often employed for power faction correction purposes. Moreover, type-1 generators limit aerodynamic power by varying the pitch angle of their blades, imposing great mechanical stress on blades, shafts and gears, demanding a robust mechanical design and preventing these generators to operate above certain wind speed (ELLIS et al., 2011).

Figure 4: Representation of Type-1 Wind Turbine Generator

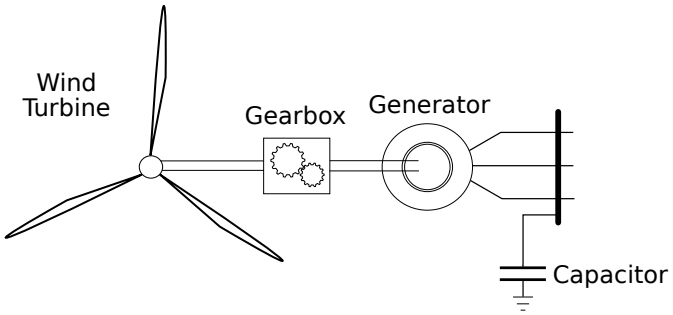

1.2.2 Type-2 Wind Turbine Generator

Similarly to Type-1 WTG, Type-2 Wind Turbine Generators are composed of an asynchronous machine connected to a wind turbine via gearbox, but, instead of SCIG, Wound Rotor Induction Generator (WRIG) are used to convert kinetic energy into electricity. The WRIG has access to its rotor windings, allowing to vary the rotor resistance. As a direct consequence, this machine can operate in different wind speeds by adjusting its torque-speed curve as needed (ELLIS et al., 2011). Therefore, Type-2 WTG have a WRIG with a variable resistance connected to its rotor terminals, as shown in Figure 5.

Figure 5: Representation of Type-2 Wind Turbine Generator

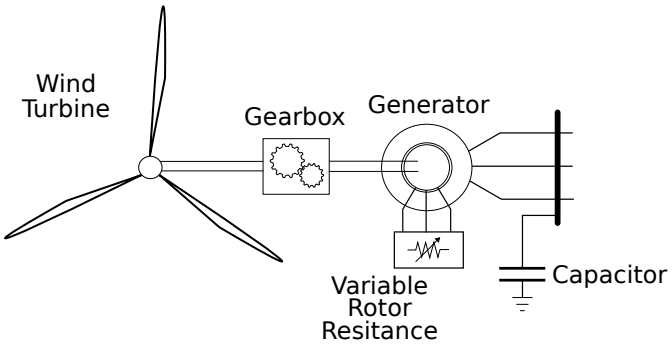

This type of generator has then three speed control systems, with rotor resistance control responding to rapid changes in speed, gearbox control for medium variations and pitch control for slow changes. These control system work together to maintain power output constant and reduce mechanical stress on components. The effects on the torque-speed curve caused by different rotor resistances are shown in Figure 6. For a fixed power, increasing rotor resistance increases the speed needed on the shaft, allowing the wind turbine to operate above rated wind speed. However, the speed range is only ±10% of rated slip. Also, this machine still needs a reactive compensation circuit on its terminals (MULJADI et al., 2010).

Figure 6: Torque-speed curve

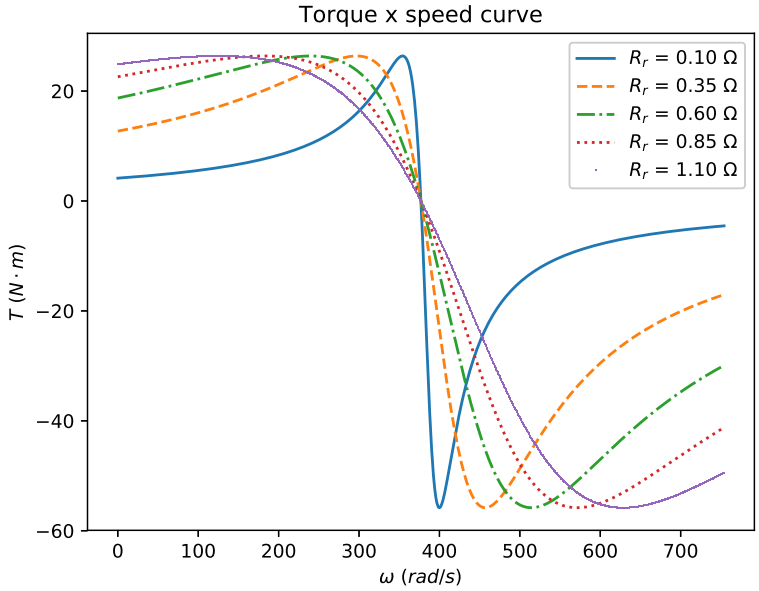

1.2.3 Type-3 Wind Turbine Generator

A Type-3 Wind Turbine Generator, often called Doubly Fed Induction Generator (DFIG), is also composed of a wound rotor machine connected to a wind turbine. But, instead of varying rotor resistance, a DFIG has its rotor supplied with AC voltage by a back-to-back frequency converter, as displayed in Figure 7. By varying the voltage frequency on the rotor circuit, the generator is able to supply power to the grid in a wider range of wind speed, reaching up to ±30% of rated slip. In addition, the converter can control both real and reactive power independently, ending the necessity of capacitors (MULJADI et al., 2010). Since approximately 30% of rated power flows through the rotor windings, power electronics components have lower specifications and don't have great impact on overall costs. On the other hand, these generators need regular maintenance due to slip rings, brushes and gearbox, preventing its use in offshore applications (YARAMASU et al., 2015).

Figure 7: Representation of Type-3 Wind Turbine Generator

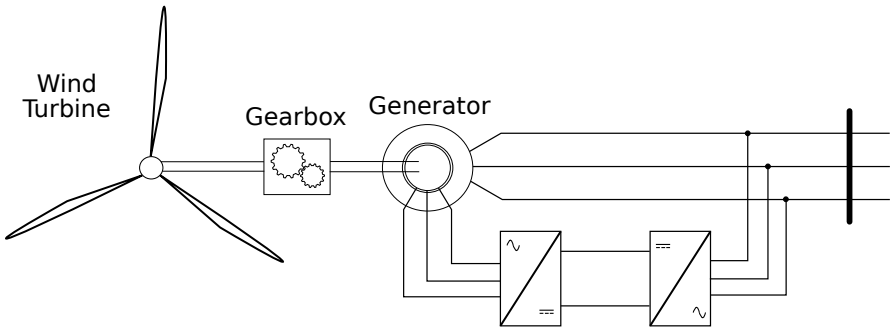

1.2.4 Type-4 Wind Turbine Generator

The last type of wind turbine generator, also called Full-Converter Generator, is composed of a electrical machine connected to the grid through a back-to-back frequency converter. The converter will operate converting the electrical frequency generated to standard, allowing this type of WTG to operate in a large range of wind speed (up to almost 100% of rated slip). Due to the converter operation, connection to the wind turbine can be made directly or via gearbox. Likewise, it allows the use of synchronous and asynchronous electrical machines as generator, with Permanent Magnet Synchronous Generator (PMSG), Electrical Excited Synchronous Generator (EESG) and SCIG being most common, because of cost and maintenance purposes. Similar to DFIG, full-converter generators are able to control real and reactive power injected into the grid. However, since all power generated must flow through the power electronics, the overall cost of these generators is usually higher (YARAMASU et al., 2015). Figure 8 depicts a typical Type-4 Wind Turbine Generator.

Figure 8: Representation of Type-4 Wind Turbine Generator

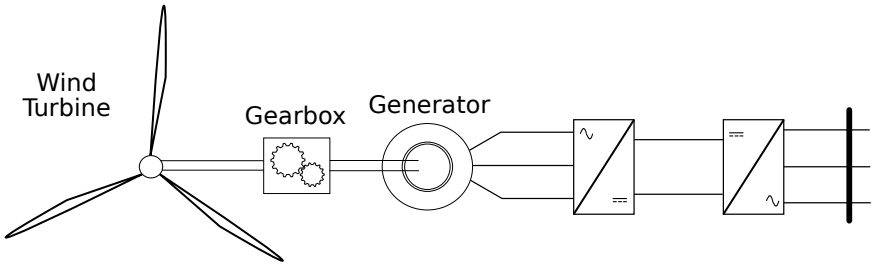

Figure 9 shows the evolution of share in installed capacity onshore for each generator type. The data shows how SCIG and WRIG lost space in the segment and how DFIG and Full-Converter Generators' participation rose, dominating the global market (MAGAGNA et al., 2017).

Figure 9: Share of installed capacity for each wind turbine generator type

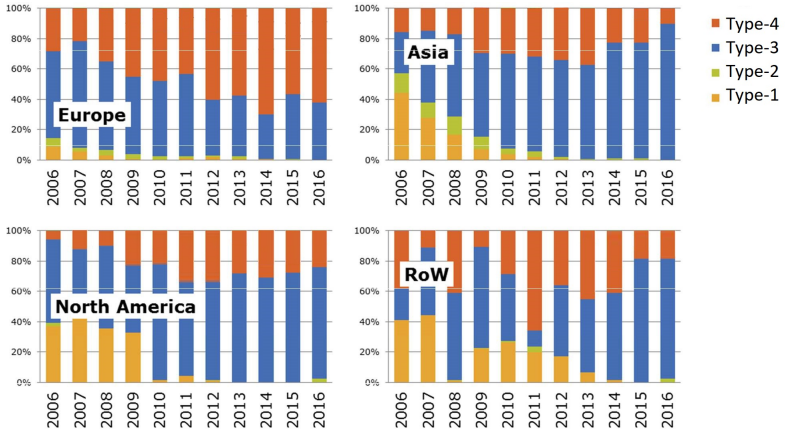

Source: JRC

In the light of the data presented above, this work aims to develop a software able to estimate the parameters of a mathematical model capable of predicting the behaviour of Type-3 Wind Turbine Generators. The DFIG mathematical model will be subject to the following chapter. Afterwards, the estimation process and methods will be presented on chapter 3. At last, expected results will be presented on chapter 5.

2 MATHEMATICAL MODEL OF TYPE-3 WIND TURBINE GENERATORS

Many mathematical models were developed during the last years that are able to represent Wind Turbine Generators of all types. All those models have in common the fact that they are based on the generic models proposed by the studies made by WECC and IEEE and presented in the last chapter. In this chapter, a few mathematical models concerning Type-3 WTG are presented and characterized and, at the end, one of them will be chosen as object of study.

2.1 Mathematical Model #1

Proposed by (ERLICH et al., 2012), this mathematical model is able to represent the dynamic of both Type-3 and -4 WTG's and can be used to simulate entire wind power plants. In this model, a Thevenin equivalent circuit is connected to grid with a controlled voltage source, as depicted in Figure 10.

Figure 10: Type-3 WTG model proposed by Erlich

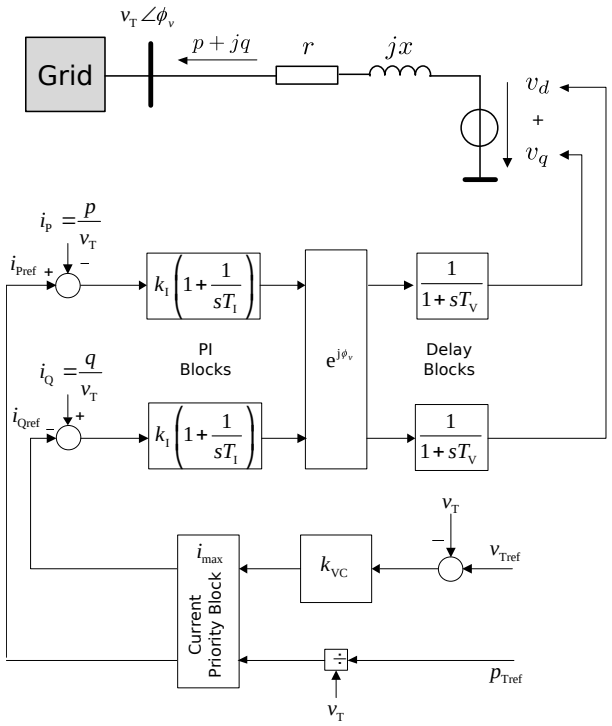

Source: Adapted from (ERLICH et al., 2012)

Terminal voltage v_T is the variable of interest in this model, appearing as input to DFIG's control system. Active and reactive current are calculated using that input,

according to equation (2.1).

$$\begin{cases} I_{Ac} = \frac{v_T}{p_{Tref}} \\ I_{Re} = k_{VC}(v_{Tref} - v_T) \end{cases} \tag{2.1}$$

The calculated currents feed a current priority block. This block analyses the current magnitude and terminal voltage level and decides whether power injection or voltage control will be prioritize. In summary, it checks if the generator's current is below a maximum level i_{max} and, if it is not, the block verifies if terminal voltage is above a threshold value v^* to decide what will be prioritized. The following algorithm describes the current priority block operation.

if $\sqrt{I_{Ac}^2 + I_{Re}^2} \leq i_{max}$ then:

$$\begin{cases} i_{Pref} = I_{Ac} \\ i_{Qref} = I_{Re} \end{cases}$$

else:

if $v_T \geq v^*$ then:

$$\begin{cases} i_{Pref} = min(i_{max}, I_{Ac}) \\ i_{Qref} = \sqrt{i_{max}^2 - i_{Pref}^2} \end{cases}$$

else:

$$\begin{cases} i_{Qref} = min(i_{max}, I_{Re}) \\ i_{Pref} = \sqrt{i_{max}^2 - i_{Qref}^2} \end{cases}$$

The following PI blocks stand for the DFIG controllers (blade, gearbox, rotor-side and grid-side converters controllers) and their outputs follow the equations presented in (2.2).

$$\begin{cases} V_{PA} = k_I[(i_{Pref} - \frac{p}{v_T}) + \frac{1}{T_I}\int_0^t (i_{Pref} - \frac{p}{v_T})dt] \\ \\ V_{QA} = k_I[(\frac{q}{v_T} - i_{Qref}) + \frac{1}{T_I}\int_0^t (\frac{q}{v_T} - i_{Qref})dt] \end{cases} \tag{2.2}$$

Until here the controller operates on terminal voltage oriented coordinates, so a coordinate transformation block is needed to adequate to synchronous grid coordinates. This block operates according to equations (2.3).

$$\begin{cases} V_{PAS} = -V_{PA}cos(\theta_v) - V_{QA}sin(\theta_v) \\ V_{QAS} = V_{PA}sin(\theta_v) - V_{QA}cos(\theta_v) \end{cases} \tag{2.3}$$

Last, two delay blocks supplying the voltage source (one for each component d and q) simulate the delay effects of the electrical machine and the back-to-back converter. Their effects are described by (2.4).

$$\begin{cases} \dot{v}_d = \frac{1}{T_V}(v_d - V_{PAS}) \\ \dot{v}_q = \frac{1}{T_V}(v_q - V_{QAS}) \end{cases} \tag{2.4}$$

The outputs of this model are real and reactive power produced (or consumed) by the WTG and their equations are shown below.

$$\begin{cases} P_e = \frac{r(v_{Td}v_d + v_{Tq}v_q - v_T^2) + x(v_{Tq}v_d - v_{Td}v_q)}{r^2+x^2} \\ Q_e = \frac{x(v_{Td}v_d + v_{Tq}v_q - v_T^2) - r(v_{Tq}v_d - v_{Td}v_q)}{r^2+x^2} \end{cases} \tag{2.5}$$

Thus, this model can be interpreted as follows:

$$\begin{cases} \dot{x} = f(x, u, y, p) \\ y = g(x, u, y, p) \end{cases} \tag{2.6}$$

where the state variables x, inputs u, outputs y and parameters p vectors are described by (2.7), (2.8), (2.9) and (2.10), respectively.

$$x = [v_d, v_q]^T \tag{2.7}$$

$$u = [v_T, \theta_v, P, Q]^T \tag{2.8}$$

$$y = [P_e, Q_e]^T \tag{2.9}$$

$$p = [r, x, k_I, T_I, T_V, k_{VC}]^T \tag{2.10}$$

In (2.10), the parameters correspond to the stator equivalent resistance r and reactance x, PI gain k_I and time constant T_I, delay block time constant T_V and voltage block gain k_{VC}.

3 ESTIMATION PROCESS

Parameter estimation problems can be interpreted as optimization problems, where one must find the optimal values of parameters in order to reduce the error between real system and model. During the years, many methods were developed to address this problem, but two approaches have been largely employed to obtain its solution.

The first approach applies metaheuristics to obtain a sufficiently good solution. These methods are used in a variety of cases, ranging from biological to engineering problems, due to the fact that they are not developed for a specific type of problem. Metaheuristics employ a stochastic search to encounter (near-)optimal solutions within a given region. However, they often take a great amount of time to converge to a solution (BLUM; ROLI, 2003). Examples of metaheuristics are Ant Colony Optimization, Differential Evolution, Particle Swarm Optimization and Genetic Algorithm. Applications of this approach in electrical power system cases can be found in (TODOROVSKI; RAJIČIĆ, 2006) and (YOSHIDA et al., 2000).

The second approach applies analytical methods to find a global/local optimum solution. These methods use equations derived from the problem to locate an optimal solution. Thus, they are problem specific and must be adapted from one case to another. Analytical methods often converge in few iterations, reducing processing time, but are sensitive to initial conditions.

In this work is proposed to combine both approaches, reducing the effects of their disadvantages and improving overall convergence. Mean-Variance Mapping Optimization (MVMO) was the metaheuristic chosen for this problem, alongside Trajectory Sensitivity Method (TS) as analytical method. Both methods will be discussed in the following sections.

The flowchart depicted in Figure 11 illustrates how the proposed method works. At first, a disturbance occurs, resulting in a dynamic response of the real system. The real system's outputs are compared to the model behaviour when the same disturbance is applied to it. The error $J(p)$ is evaluated and while it is greater than a given tolerance t_1, MVMO algorithm will search for a local solution. Afterwards, the error will eventually drop to a value lower than t_1, and TS will be used to refine the search to a optimal solution, with error level below t_2. The error will be evaluated through the Least-Squares Method, given by equation 3.1, where y_r and y stand for the real system and model outputs.

$$J(p) = \frac{1}{2}\int_0^{T_0} (y_r(t) - y(t))^T (y_r(t) - y(t)) dt \tag{3.1}$$

Figure 11: Flowchart of estimation method

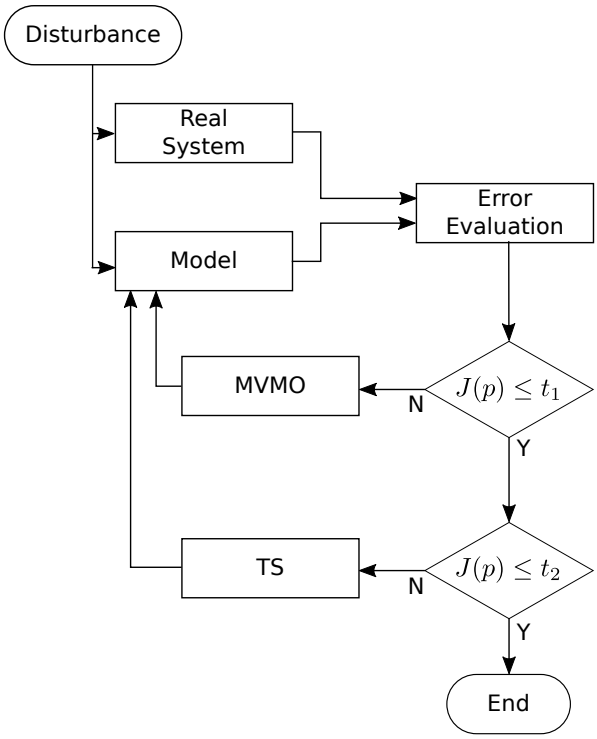

3.1 Mean-Variance Mapping Optimization

Presented in (ERLICH; VENAYAGAMOORTHY; WORAWAT, 2010), this population-based metaheuristic shares characteristics with other evolutionary algorithms, but differ from them on how to induce mutations on the offspring in order to diversify the population. By considering statistical data of population during mutation process, MVMO introduces a memory factor to it, enhancing search mechanism. Due this factor, MVMO performs better than similar metaheuristics when population size is relatively small (NAKAWIRO; ERLICH; RUEDA, 2011). In this section, the terms 'gene', 'individuals' and 'population' will be used instead of 'parameter', 'parameter vector' and 'set of vectors' for the sake of analogy.

Before the search process starts, a few settings must be done, such as population size, number of offspring, number of genes selected for mutation and selection method. Also, the search region is defined by setting the range within genes can vary. This constrains their values within a feasible region, preventing divergence. The search region is later normalized for all genes, aiding the process. Termination criteria is also set in this step. In this work, both number of generations and fitness will be used as stop criteria.

With all set, a randomly-distributed population is generated, evaluated and sorted. Moreover, the mean and variance of every gene are calculated. These values will later be used on the mutation process. The individual with better fitness is selected as parent

from whom new individuals will evolve. The offspring is then created following three steps common in evolutionary algorithms: gene selection, mutation and crossover. After creation, the offspring is introduced to the population and the worst individual is discarded, as depicted in Figure 12.

Figure 12: Exemplification of MVMO process

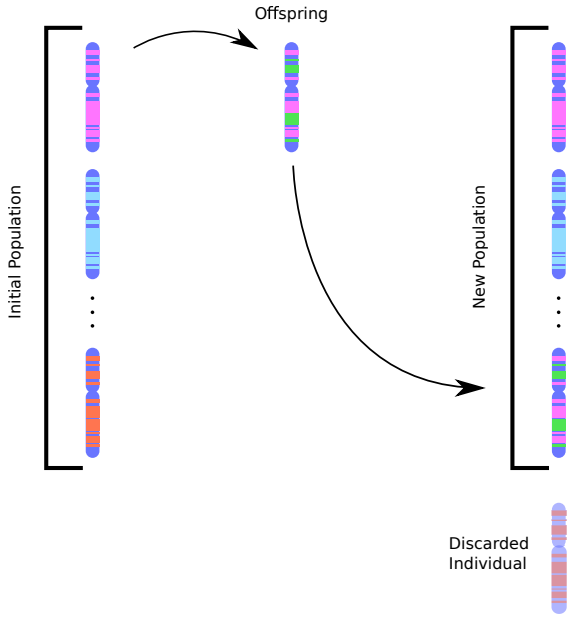

Gene selection can be done in many ways and even vary throughout the estimation process, with strategies' efficiency depending on the problem. However, three strategies are commonly used in this step. The first one is comprised of randomly selecting which genes will suffer mutation and which will be directly inherited from the parent. Gene selection can also be done by a moving window approach or even a combination of both strategies, with part of the genes selected at random and other through the window.

Mutation step takes place right after gene selection. At first, each selected gene receives a random value x_i' between [0,1] that will be used as an input to a mapping function based on the mean and variance of each particular gene on the population. Variance v_i will directly influence on the shape factor given by (3.2), where f_s is the scaling factor responsible for focusing on exploration or exploitation. In the event of zero variance, the last non-null value of v_i is used.

$$s_i = -f_s ln(v_i) \tag{3.2}$$

Shape factor and mean value of gene are used as inputs to a transformation function h, detailed in (3.3). The final value of the gene is obtained through the mapping function described by equation (3.4), where $h_x = h(u_i = x_i')$, $h_1 = h(u_i = 1)$ and $h_0 = h(u_i = 0)$.

It is important to notice that the mapping function will always provide a result in the interval [0,1], not violating the normalization made at beginning.

$$h(\bar{x}_i, s_{i1}, s_{i2}, u_i) = \bar{x}_i(1 - e^{-u_i s_{i1}}) + (1 + \bar{x}_i)e^{-(1-u_i)s_{i2}} \tag{3.3}$$

$$x_i = h_x + (1 - h_1 + h_0)x'_i - h_0 \tag{3.4}$$

The resulting mapping function is depicted in Figure 13. The effects of different mean and shape factor values can be observed on Figure 14.

Figure 13: Example of MVMO mapping function

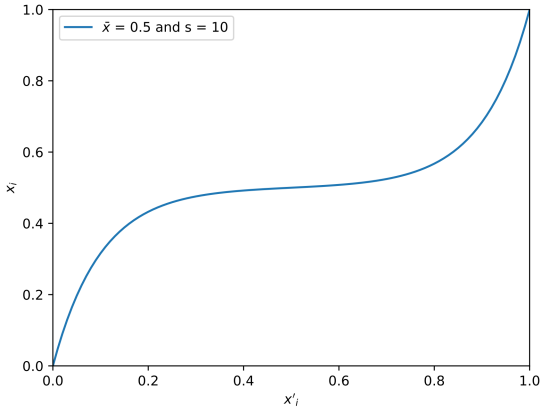

Figure 14: Effect of different mean and shape factor values on the mapping function

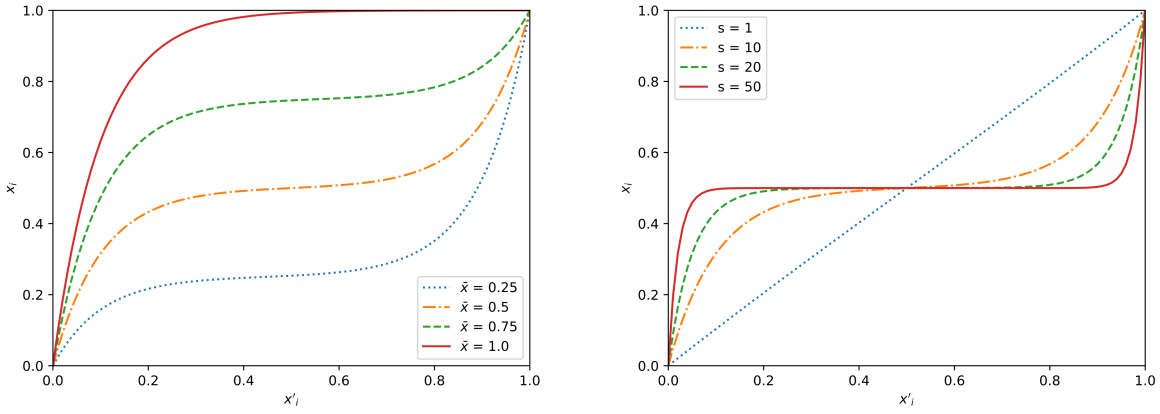

As shown in (3.3), two shape factors are used to evaluate the function. Different values of shape factors emphasizes the search below or above mean value. Thus, by controlling the values s_{i1} and s_{i2}, the method can prioritize exploitation or exploration

on a given region. Figure 15 depicts how asymmetrical shape factors affect the mapping function.

Figure 15: Comparison between symmetrical and asymmetrical shape factors

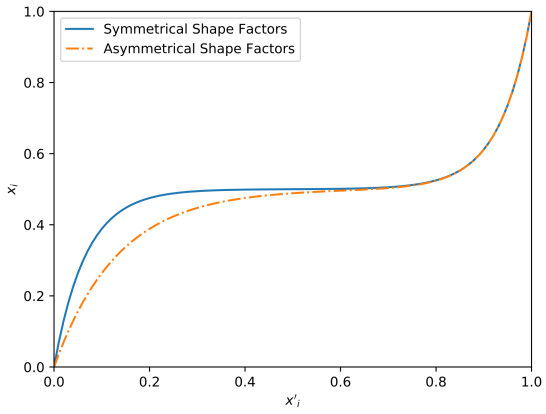

The final step during offspring generation is crossover. During this phase, the mutated genes are united with the remaining genes inherited from parent, forming the new individual. This new individual is evaluated and included to the population if it is better than, at least, the population's worst individual. This process goes on until at least one stop criterion has been fulfilled.

The main advantages of this method are low computational cost, good performance using small populations, constrained search region, preventing divergence, and the fact that it is non-specific. On the other hand, this method, as other metaheuristics, takes a great amount of time to converge when its error approaches zero.

3.2 Trajectory Sensitivity Method

Considering a nonlinear system described by (2.6), in order to minimize the error between model and real system, given by (3.1), one must discover a parameter vector p^* such as:

$$G(p^*) = \frac{\partial J(p^*)}{\partial p} = 0 \tag{3.5}$$

Truncating the Taylor series for $G(p)$ on the first-order term results on (3.6). The variable Γ is described in (3.7).

$$G(p^*) = G(p) + \Gamma(p)(p^* - p) \tag{3.6}$$

$$\Gamma(p) = \frac{\partial G}{\partial p} \approx \int_0^{T_0} \left(\frac{dy}{dp}\right)^T \left(\frac{dy}{dp}\right) dt \tag{3.7}$$

By rearranging the terms on (3.6), the following equation is obtained. It describes how the parameters are updated after the n^{th} iteration.

$$p^{n+1} = p^n + \Gamma^{-1}(p^n) \cdot G(p^n) \tag{3.8}$$

The partial derivatives (also called trajectory sensitivities) $\frac{\partial y}{\partial p}$, used directly in (3.7) and indirectly in (3.5), can be approximated by the difference shown in (3.9). The outputs y^1 and y^0 are obtained using parameter vectors p^1 and p^0, respectively, and $\Delta p = p^1 - p^0$. Using (3.9) allows Trajectory Sensitivity method to be applied on both differentiable and non-differentiable systems (BENCHLUCH; CHOW, 1993).

$$\frac{\partial y}{\partial p} \approx \frac{y^1 - y^0}{\Delta p} \tag{3.9}$$

The Trajectory Sensitivity Method has fast convergence characteristics and can applied directly to nonlinear problems, not requiring linearization. Also, by analyzing the sensitivities, the method provides information about parameters' identifiability. However, TS is very sensitive to initial value of parameter chosen as start point. Thus, if the initial values are too far from real, the method can either diverge or converge to values. Besides, the information provided to the method must contain the effects of the parameters, otherwise they won't be observable (BENCHLUCH; CHOW, 1993).

By associating MVMO and TS, the hybrid estimation approach proposed in this work combines most benefits of both methods whilst mitigating their disadvantages. The resulting method has smaller convergence time when compared to MVMO alone and is less sensitive than TS to initial values of parameters, improving its performance.

4 SOFTWARE CONCEPT

NICE

5 EXPECTED RESULTS

The expected result of this work is a software capable of correctly estimating the parameters of Type-3 WTG's mathematical model. To do so, the software will apply the proposed estimation method comprises of MVMO and TS methods combined.

The real model behaviour will be obtained through simulation on specific software, such as DIgSILENT or MATLAB, and real data, if available. At first, Erlich's model will be employing, but it can be further changed if needed. Also, other estimation methods, such as PSO, ED or Kalman Filters, may be implemented and their performance compared.

The hybrid approach for parameters estimation presented in this work is already implemented and have shown great results for models. As depicted in Figure **??**, the proposed method can correctly identify the parameters of a spring-mass system. The same application was employed on load model identification and is subject of a paper presented by the author on the 2019 Canadian Conference on Electrical and Computer Engineering.

BIBLIOGRAPHY

ABEEOLICA. **Annual Wind Energy Report**. Sao Paulo, 2018.

AMARANTE, O. A. C. do et al. **Atlas do Potencial Eólico Brasileiro**. Brasilia, 2001.

ANEEL. **Atlas de Energia Elétrica do Brasil**. Brasilia, 2005. Disponível em: <http://www.aneel.gov.br/livros/-/asset{_}publisher/eZ674TKh9oF0/content/atlas-de-energia-eletrica-do-brasil/656>.

ASMINE, M. et al. Model Validation for Wind Turbine Generator Models. **Power Systems, IEEE Transactions on**, v. 26, n. 3, p. 1769–1782, 2011. ISSN 0885-8950.

BENCHLUCH, S. M.; CHOW, J. H. A Trajectory Sensitivity Method for the Identification of Nonlinear Excitation System Models. **IEEE Transactions on Energy Conversion**, v. 8, n. 2, p. 159–164, jun 1993. ISSN 15580059. Disponível em: <http://ieeexplore.ieee.org/document/222699/>.

BLUM, C.; ROLI, A. Metaheuristics in Combinatorial Optimization: Overview and Conceptual Comparison. **ACM Computing Surveys**, v. 35, n. 3, p. 268–308, sep 2003. ISSN 0360-0300. Disponível em: <http://portal.acm.org/citation.cfm?doid=937503.937505>.

Commission European. **A strategy for smart, sustainable and inclusive growth**. Brussels, 2010. 1–37 p. Disponível em: <https://www.eea.europa.eu/policy-documents/com-2010-2020-europe-2020>.

COUNCIL, W. E. C. Wecc wind power plant power flow modeling guide. **WECC Wind Generator Modeling Group, Tech. Rep**, 2008.

ELLIS, A. et al. Generic models for simulation of wind power plants in bulk system planning studies. **IEEE Power and Energy Society General Meeting**, p. 1–8, 2011. ISSN 19449925.

EPE. **Anuário Estatístico de Energia Elétrica 2018 no ano base de 2017**. Rio de Janeiro, 2018. 249 p. Disponível em: <http://www.epe.gov.br/sites-pt/publicacoes-dados-abertos/publicacoes/PublicacoesArquivos/publicacao-160/topico-168/Anuario2018vf.pdf>.

ERLICH, I. et al. Determination of Dynamic Wind Farm Equivalents using Heuristic Optimization. **Power and Energy Society General Meeting, IEEE**, p. 1–8, 2012.

ERLICH, I.; VENAYAGAMOORTHY, G. K.; WORAWAT, N. A Mean-Variance Optimization algorithm. **2010 IEEE World Congress on Computational Intelligence, WCCI 2010 - 2010 IEEE Congress on Evolutionary Computation, CEC 2010**, n. February, p. 1–6, 2010.

Federative Republic of Brazil. **Lei 10438/2002**. Brasilia: [s.n.], 2002. 1–21 p. Disponível em: <http://www.planalto.gov.br/ccivil{_}03/leis/2002/L10438.htmhttp://www.planalto.gov.br/ccivil{_}03/LEIS/2002/L104>.

MAGAGNA, D. et al. **Supply chain of renewable energy technologies in Europe: An analysis for wind, geothermal and ocean energy**. [s.n.], 2017. ISSN 1831-9424. ISBN 978-92-79-74281-1. Disponível em: <https://ec.europa.eu/jrc/en/publication/eur-scientific-and-technical-research-reports/supply-chain-renewable-energy-technologies-europe-analysis-wind-geothermal-and-ocean-energy>.

MULJADI, E.; ELLIS, A. Validation of wind power plant models. **IEEE Power and Energy Society 2008 General Meeting: Conversion and Delivery of Electrical Energy in the 21st Century, PES**, p. 1–7, 2008. ISSN 1932-5517.

MULJADI, E. et al. Short circuit current contribution for different wind turbine generator types. In: **IEEE PES General Meeting, PES 2010**. IEEE, 2010. p. 1–8. ISBN 9781424483570. Disponível em: <http://ieeexplore.ieee.org/document/5589677/>.

NAKAWIRO, W.; ERLICH, I.; RUEDA, J. L. A novel optimization algorithm for optimal reactive power dispatch: A comparative study. **2011 4th International Conference on Electric Utility Deregulation and Restructuring and Power Technologies (DRPT)**, n. 1, p. 1555–1561, 2011. ISSN 0278-0046. Disponível em: <http://ieeexplore.ieee.org/document/5994144/>.

TODOROVSKI, M.; RAJIČIĆ, D. An initialization procedure in solving optimal power flow by genetic algorithm. **IEEE Transactions on Power Systems**, v. 21, n. 2, p. 480–487, 2006. ISSN 08858950.

Wind Europe. Wind energy in Europe in 2018: Trends and statistics. **Wind Europe. (2019). Wind energy in Europe in 2018: Trends and statistics.**, 2019. ISSN 0309524X.

YARAMASU, V. et al. High-power wind energy conversion systems: State-of-the-art and emerging technologies. **Proceedings of the IEEE**, v. 103, n. 5, p. 740–788, may 2015. ISSN 00189219. Disponível em: <http://ieeexplore.ieee.org/document/7109820/>.

YOSHIDA, H. et al. A Particle swarm optimization for reactive power and voltage control considering voltage security assessment. **IEEE Transactions on Power Systems**, 2000. ISSN 08858950.